

Quantum Chemical Study on Stability and Reactivity of 1-Aminocyclopropane-1-carboxylic Acid Amine Radical Cation

Mika Ito[*1,2,3] **and Hiroaki Tokiwa**[*3]

[1]Graduate School of Human Development and Environment, Kobe University, 3-11, Tsurukabuto, Nada, Kobe 657-8501

[2]CREST, Japan Science and Technology Agency

[3]Department of Chemistry, Faculty of Science, Rikkyo University, 3-34-1 Nishi-Ikebukuro, Toshima-ku, Tokyo 171-8501

Received January 5, 2007; E-mail: ito@insilico.h.kobe-u.ac.jp

The stability and reactivity of the 1-aminocyclopropane-1-carboxylic acid (ACC) amine radical cation, which is a key intermediate of ethylene biosynthesis in plants, were examined by quantum chemical calculations. The local interactions to stabilize radical species were treated with a hydrated cluster. Potential energy curves were obtained for two types of reactions from ACC amine radical cation: (1) direct ring opening of ACC amine radical cation, followed by proton abstraction from the amino group, and (2) proton abstraction from the amino group, followed by ring opening of ACC aminyl radical. A remarkable difference was found in the ring-opening processes of reactions (1) and (2). Rate constants (k) of 6.10×10^{12} and 8.89×10^{9} s^{-1} at 298.15 K were estimated for the ring openings of ACC amine radical cation and ACC aminyl radical, respectively, at the B3LYP/6-31+G(d,p) level, and were in agreement with experimental results. The ring opening of ACC amine radical cation was 10^3-fold faster than that of ACC aminyl radical with almost no barrier height. It was thus quantitatively demonstrated that reaction (1) was more favorable than reaction (2) for ethylene synthesis.

The phytohormone ethylene is a familiar simple olefin and regulates many physiological processes in plant growth and development, such as fruit ripening.[1–3] In addition, this small molecule is the only volatile phytohormone and thus plays various vital roles through plant–plant, plant–herbivore, and plant–carnivore interactions.[4,5] As ecological studies on ethylene have accumulated, postharvest physiologists have focused efforts on delaying fruit ripening and flower fading by reducing ethylene production, and studies of ethylene biosynthesis have been undertaken to address this goal.[2,3]

Once 1-aminocyclopropane-1-carboxylic acid (ACC) was first established as a crucial precursor of the final stage of ethylene biosynthesis in plants by Adams and Yang,[6] the enzymatic conversion of ACC to ethylene has received much attention.[7–14] Many efforts have been made to assay the ethylene-forming enzyme (EFE) and to determine the genes encoding it. Hamilton et al. discovered that pTOM13 clone represents the gene encoding EFE and that the EFE catalyzes oxidation of ACC.[9,10] EFE is now called 1-aminocyclopropane-1-carboxylic acid oxidase (ACCO).[11,12] On the basis of a comparison of homologous protein sequences, ACCO has been classified as a member of a family of non-heme iron proteins.[12] The family of non-heme iron proteins is unstable, and thus, ACCO is difficult to isolate with its activity intact. Consequently, studies on ethylene biosynthesis have been challenging.[12] To the best of our knowledge, the crystal structure of the ACCO complex with ACC has not been reported, and thus, the precise mechanism of ethylene biosynthesis remains a long-standing question.

In an early experimental study, Pirrung[7] has reported that the fragmentation of ACC to ethylene occurs not by a concerted process but by a stepwise process through sequential transfers of single electrons that involve various radical species, as observed in apple tissue. Pirrung et al.[13,14] have determined ACC amine radical cation to be a key intermediate in the ACCO active site. From their experiments, they have proposed two types of reactions from the key intermediate (Scheme 1): (1) direct ring opening of ACC amine radical cation, followed by proton abstraction from the amino group (Path A in

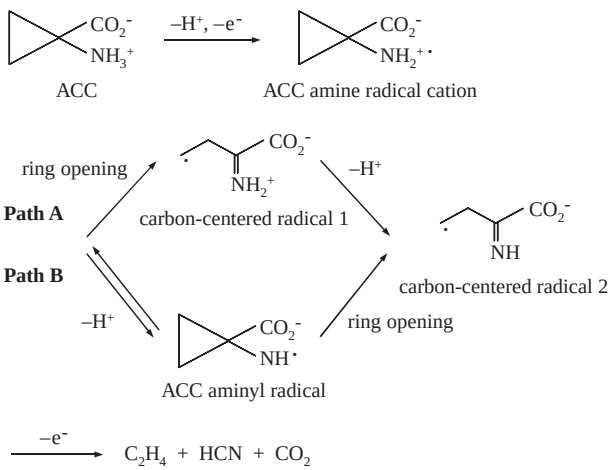

Scheme 1. Proposed reaction paths for ethylene biosynthesis from ACC.[37]

Published on the web September 13, 2007; doi:10.1246/bcsj.80.1731

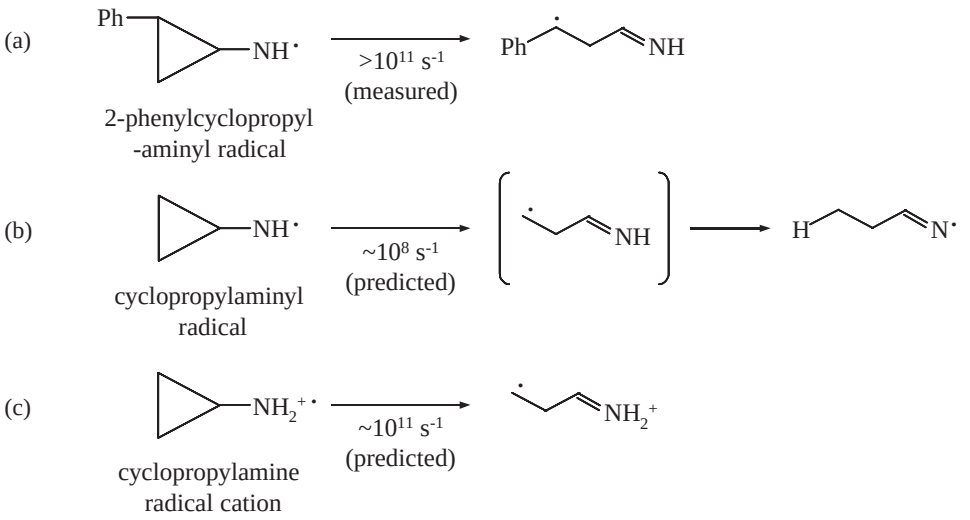

Scheme 2. Reactions of cyclopropyl radical species.

Scheme 1), and (2) proton abstraction from the amino group, followed by ring opening of ACC aminyl radical (Path B in Scheme 1). ACC amine radical cation and ACC aminyl radical are analogous to other radical species, which undergo rapid rearrangements.[15–18] To date, rate constants (k) of the ring openings of ACC amine radical cation and ACC aminyl radical have not been measured, because kinetic measurements of these ring openings have been unavailable.[13,14] On the other hand, it is known that the ring opening of 2-phenylcyclopropylaminyl radical (Scheme 2a) occurs with $k > 10^{11}\,s^{-1}$ at 293.15 K in solution[16] and, based on the known effects of the phenyl group on ring-opening rates, the ring opening of the unsubstituted cyclopropylaminyl radical (Scheme 2b) should occur with a predicted k of $\approx 10^8\,s^{-1}$.[13,14] It is also known that amine radical cations (Scheme 2c) can undergo rearrangements up to 10^3-fold faster than their cognate aminyl radicals (Scheme 2b).[15] In addition, from an experimental study on ring opening of radical species by using electron spin resonance (ESR), the ring opening of cyclopropylaminyl radical (Scheme 2b) leads quickly to internal H-atom transfer from NH group to generate iminyl radical, which would not be competent in ethylene production, whereas cyclopropylamine radical cation (Scheme 2c) produces a stable carbon-centered radical.[17] Therefore, Pirrung et al.[13,14] have suggested that reaction (1) would be more favorable than reaction (2), and the ring opening of ACC amine radical cation should occur with $k > 10^8\,s^{-1}$. On the other hand, the pH environment of the active site of the enzyme is unknown, and the amine radical cation and the aminyl radical differ only by protonation, with $pK_a \approx 7$ for dialkylaminyl radicals.[15] On the basis of this fact, Pirrung et al.[13,14] have also suggested that it is difficult to exclude ACC aminyl radical as a possible early intermediate in ethylene biosynthesis.

In spite of much effort to elucidate the mechanism of ethylene biosynthesis, details of the stability and reactivity of ACC amine radical cation are still unclear, since the relevant information on reactions of short-lived radical species is obtained only by product analysis in experimental studies. On the other hand, by taking advantage of quantum chemical methods, such as the ab initio molecular orbital (MO) methods, we can analyze details of structures, properties, and reactions of radical species, as well as of those of other molecular species. In our previous study,[19] the proton-transfer mechanism for ionization of the hydrated cluster of ACC has been investigated by the ab initio MO method. We have shown that local interactions between ACC and water molecules are necessary to fully stabilize the zwitterionic form of ACC and have found that the neighboring water molecules directly participate in the ionization process of ACC. We have thus concluded that water molecules interacting directly with ACC may significantly contribute to the reaction that forms ethylene from ACC in aqueous solution. As well as ACC precursor, ACC amine radical cation intermediate has a zwitterionic form. We therefore suggest the detailed analysis of the stability and reactivity of ACC amine radical cation in aqueous solution, including the effects of local interactions between ACC amine radical cation and water molecules, should be performed to better understand ethylene biosynthesis in plants.

In this work, the stability and reactivity of ACC amine radical cation in aqueous solution were investigated by quantum chemical calculations as a first step in the investigation of ethylene biosynthesis. A hydrated cluster model was used to include the effects of the local interactions of ACC amine radical cation with water molecules in aqueous solution. In this investigation, the proposed two types of reactions, i.e., reactions (1) and (2) from ACC amine radical cation (Path A and Path B before an electron transfer in Scheme 1), were particularly focused on and compared them with each other. To better understand how ethylene synthesis proceeds in plants, it is important to clarify which reaction path is more favorable for ethylene synthesis in aqueous solution. We should note that the analysis of the ethylene release process, which requires an electron transfer from the solute (carbon-centered radical 2 in Scheme 1) to the active center of the enzyme, is beyond the scope of the current investigation, because the electron transfer is difficult to analyze in the model system without the enzymatic environment. To ultimately elucidate the mechanism of the entire ethylene biosynthesis, the effects of the en-

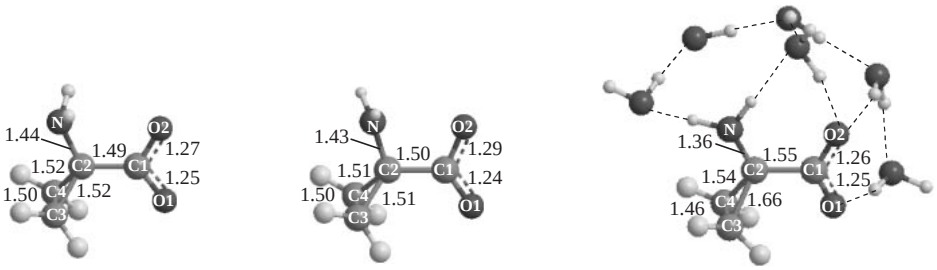

1a **1b** **1c**

Fig. 1. Optimized geometries of ACC amine radical cation in (**1a**) the isolated system, (**1b**) the dielectric continuum medium using PCM, and (**1c**) the hydrated cluster at the B3LYP/6-31+G(d,p) level. Bond lengths are shown in Å.

zymatic environment should be included in further studies. However, the findings obtained from this work are of importance for eventually understanding how ethylene is created in plants.

Computational Methods

Density functional theory (DFT) methods have recently been used for various systems and have yielded promising results for many molecular systems. In particular, systematic studies of hydrogen-bonded systems have verified that DFT reasonably describes the thermodynamic characteristics of hydrogen bonding as long as reliable basis sets are used.[20–22] Therefore, one of the DFT methods, the B3LYP method, which is the Becke's three-parameter hybrid method using the LYP local and non-local exchange functionals of Lee, Yang, and Parr, was used.[23–25] The second-order Møller–Plesset perturbation (MP2) method[26–28] was also used. The spin multiplicities were doublet, and the sum of Mulliken spin densities was calculated to be 1 for all compounds. In the present calculations, the 6-31+G(d,p) basis set was used.[29,30] All structures were optimized at the B3LYP/6-31+G(d,p) level. Because converging the optimization using the MP2 is difficult, single-point MP2 calculations were performed using the structures optimized with the B3LYP method. The B3LYP results were compared with the MP2 results when necessary. To verify that each critical point was at an energy minimum, vibrational analysis based on the analytical second-derivative method was used for all optimized geometries. One imaginary frequency for transition-state (TS) structures and zero for equilibrium structures were confirmed by the normal coordinate analysis. Intrinsic reaction coordinate (IRC) analysis[31] on all of the reactions was performed using the B3LYP method to confirm the nature of TSs. The structures and energies of the B3LYP results will be discussed, unless otherwise noted.

Short-range solvent effects were taken into account by using a hydrated cluster model including six water molecules, since short-range local ACC–water interactions were satisfactorily modeled by the ACC$\cdot(H_2O)_6$ cluster as shown in our previous paper.[19] Long-range solvent effects were taken into account by means of a dielectric continuum medium by using the polarized continuum model (PCM).[32] For the dielectric continuum medium, $\varepsilon = 78.5$ was used as the dielectric constant in water. All calculations were carried out using the Gaussian98 program package.[33]

Results and Discussion

Stability of ACC Amine Radical Cation. Quantum chemical calculations were used to investigate the stability of ACC amine radical cation, which has the amine-radical-cation and zwitterionic forms at the same time. At the beginning of this investigation, the structural features of the ACC amine radical cation were analyzed in various environments. The three optimized structures of ACC amine radical cation are shown in Fig. 1. Structures **1a**, **1b**, and **1c** were obtained in the isolated system, the dielectric continuum medium using PCM, and the hydrated cluster, respectively, by the B3LYP method. Table 1 shows the Mulliken atomic spin densities and the Mulliken atomic charges of these species calculated by the B3LYP and MP2 methods.

Structures **1a**, **1b**, and **1c** were almost the same except for the orientation of the hydrogen atom as shown in Fig. 1, but they had different atomic spin densities and charges as shown in Table 1. Structure **1a** was obtained without a radical on nitrogen atom **N** of the amino group, and there were low atomic spin densities on **N** (0.12 and 0.01 at the B3LYP/6-31+G(d,p) and MP2/6-31+G(d,p) levels, respectively). In addition, structure **1a** was obtained with a radical on oxygen atom **O1** of the carboxyl group (Table 1). In contrast, structures **1b** and **1c** were obtained with high atomic spin densities on **N** (0.59) by the B3LYP method. Single-point MP2 calculations yielded atomic spin densities on **N** of 0.04 and 0.90 for structures **1b** and **1c**, respectively, indicating that only structure **1c** has a radical on **N**. The calculated charges on NH_2 of the amino group for structures **1a**, **1b**, and **1c** were +0.06, +0.34, and +0.38, respectively, by the B3LYP method. The MP2 calculations yielded charges on NH_2 of the amino group of 0.00, −0.09, and +0.53 for structures **1a**, **1b**, and **1c**, respectively, indicating that only structure **1c** has a cation on NH_2. These calculations of atomic spin densities on **N** and charges on NH_2 show that only structure **1c** corresponds to the amine-radical-cation form. In addition, total charges of **O1** and **O2** of the carboxyl group were calculated. The negative charges calculated for structure **1c** of −1.28 and −1.59 by the B3LYP and MP2 methods, respectively, were larger than the negative charges calculated for structures **1a** (−0.68 and −0.74) and **1b** (−1.09 and −0.83). These charge values on the hydrophilic groups show that only structure **1c** corresponds to the zwitterionic form.

From these results, the local interactions between water

Table 1. Atomic Spin Densities and Atomic Charges of Structures **1a**, **1b**, and **1c** Obtained in the Isolated System, the Dielectric Continuum Medium Using PCM, and the Hydrated Cluster, Respectively, Calculated by the B3LYP and MP2 Methods with the 6-31+G(d,p) Basis Set

		B3LYP/6-31+G(d,p)			MP2/6-31+G(d,p)[a)]		
		1a	**1b**	**1c**	**1a**	**1b**	**1c**
Spin density	**N**	0.12	0.59	0.59	0.01	0.04	0.90
	C1	−0.07	−0.01	0.01	−0.13	−0.16	0.04
	C2	−0.01	−0.06	0.02	0.04	0.07	−0.25
	C3	0.00	0.03	0.33	0.00	0.00	0.43
	C4	0.00	0.01	0.05	0.00	−0.01	0.02
	O1	0.48	0.18	0.05	0.99	0.98	0.02
	O2	0.49	0.31	−0.01	0.10	0.09	−0.01
Charge[b)]	**N**	0.06	0.34	0.38	0.00	−0.09	0.53
	C1	0.28	0.42	0.23	0.41	0.47	0.61
	C2	0.00	0.03	0.31	0.05	0.26	0.19
	C3	0.17	0.16	0.18	0.14	0.10	0.16
	C4	0.17	0.14	0.18	0.14	0.08	0.10
	O1	−0.35	−0.57	−0.59	−0.15	−0.15	−0.74
	O2	−0.33	−0.52	−0.69	−0.59	−0.68	−0.85

a) The single point MP2 calculations using the optimized geometries in the hydrated cluster by the B3LYP calculations. b) The atomic charges with hydrogens summed into heavy atoms.

molecules and ACC amine radical cation are necessary for the representation of the character of ACC amine radical cation and for the analysis of the reactions of ACC amine radical cation. In light of this finding, the hydrated cluster was adopted to probe how the reactions of ACC amine radical cation proceed.

Reactivity of ACC Amine Radical Cation. The calculations were performed for the proposed two types of reactions from ACC amine radical cation using the hydrated cluster: (1) the direct ring opening of ACC amine radical cation, followed by the proton abstraction from the amino group (Path A in Scheme 1) and (2) the proton abstraction from the amino group, followed by the ring opening of ACC aminyl radical (Path B in Scheme 1). Figure 2 shows the optimized geometries of the reactant (**RC**), transition-state (**TS**), and intermediate (**INT**) species for (a) Path A and (b) Path B in the hydrated cluster by the B3LYP method. Tables 2 and 3 show the atomic spin densities and the atomic charges of these species for Path A and Path B calculated by the B3LYP method, respectively, and Tables 4 and 5 show those for Path A and Path B calculated by the MP2 method, respectively. Figure 3 shows the potential energy curves for Path A and Path B in the hydrated cluster by the B3LYP method. Details of Path A and Path B are shown in following sections.

Structural Changes: Firstly, the structural change of Path A was analyzed. As shown in Fig. 2a, one side of the cyclopropane ring of **RC** opens to give **INT1a** via **TS1a** ($284i$ cm^{-1}), and subsequently a proton of the amino group of the **INT1a** transfers to a water molecule **W1**, and three protons of **W1**, **W2**, and **W3** transfer to give **INT2a** via **TS2a** ($816i$ cm^{-1}). A single TS (**TS2a**) for this water-assisted proton transfer indicates that the four protons move in a concerted fashion via the hydrogen-bonding network in the hydrated cluster. Caused by this proton-transfer process, an oxonium ion is formed at **W4** in **INT2a**. From **RC** to **INT1a**, the C2–N bond shortened from 1.36 to 1.29 Å, indicating that a double bond is formed at the C2–N bond caused by the ring opening. Through these ring-opening and proton-transfer processes, a marked structural change appeared in the C2–C3 bond of the solute. From **RC** to **INT2a**, the C2–C3 bond gradually lengthened from 1.66 to 2.47 Å caused by the first ring-opening process. To analyze the electronic aspect of the solute, the atomic spin densities and the atomic charges of the solute were calculated as shown in Tables 2 and 4. The highest spin density was obtained at **N** of **RC**, **C3** of **TS1a**, **C3** of **INT1a**, **C3** of **TS2a**, and **C3** of **INT2a** in the atoms of the each structure of Path A, indicating that a radical is formed at these atoms. The charges of **N** of **INT1a** were positive (+0.35 and +0.39 the B3LYP/6-31+G(d,p) and MP2/6-31+G(d,p) levels, respectively), whereas those of **N** of **INT2a** were negative (−0.21 and −0.22 at the B3LYP/6-31+G(d,p) and MP2/6-31+G(d,p) levels, respectively), indicating that the cation on the amino group of the solute is lost by the proton transfer.

Secondly, the structural change of Path B was analyzed. As shown in Fig. 2b, a proton of the amino group of **RC** transfers to a water molecule **W1**, and three protons of **W1**, **W2**, and **W3** concertedly transfer to give **INT1b** via **TS1b** ($953i$ cm^{-1}), and subsequently, one side of the cyclopropane ring of **INT1b** opens to give **INT2b** via **TS2b** ($486i$ cm^{-1}). Caused by this proton-transfer process, an oxonium ion is formed at **W4** in **INT1b**, **TS2b**, and **INT2b**. From the **INT1b** to **INT2b**, the C2–N bond shortened from 1.39 to 1.28 Å, indicating that a double bond is formed at the C2–N bond caused by the ring opening. Through these proton-transfer and ring-opening processes, a notable structural change appears in the C2–C3 bond of the solute. From **RC** to **INT1b**, the C2–C3 bond gradually shortened from 1.66 to 1.58 Å caused by the proton transfer, and from **INT1b** to **INT2b**, it lengthened from 1.58 to 2.49 Å caused by the ring opening. It was shown that the C2–C3 bond of **INT1b** was calculated to be shorter than that of **RC** by 0.08 Å, indicating that the C2–C3 bond of **INT1b** is stronger than that of **RC**. The atomic spin densities and

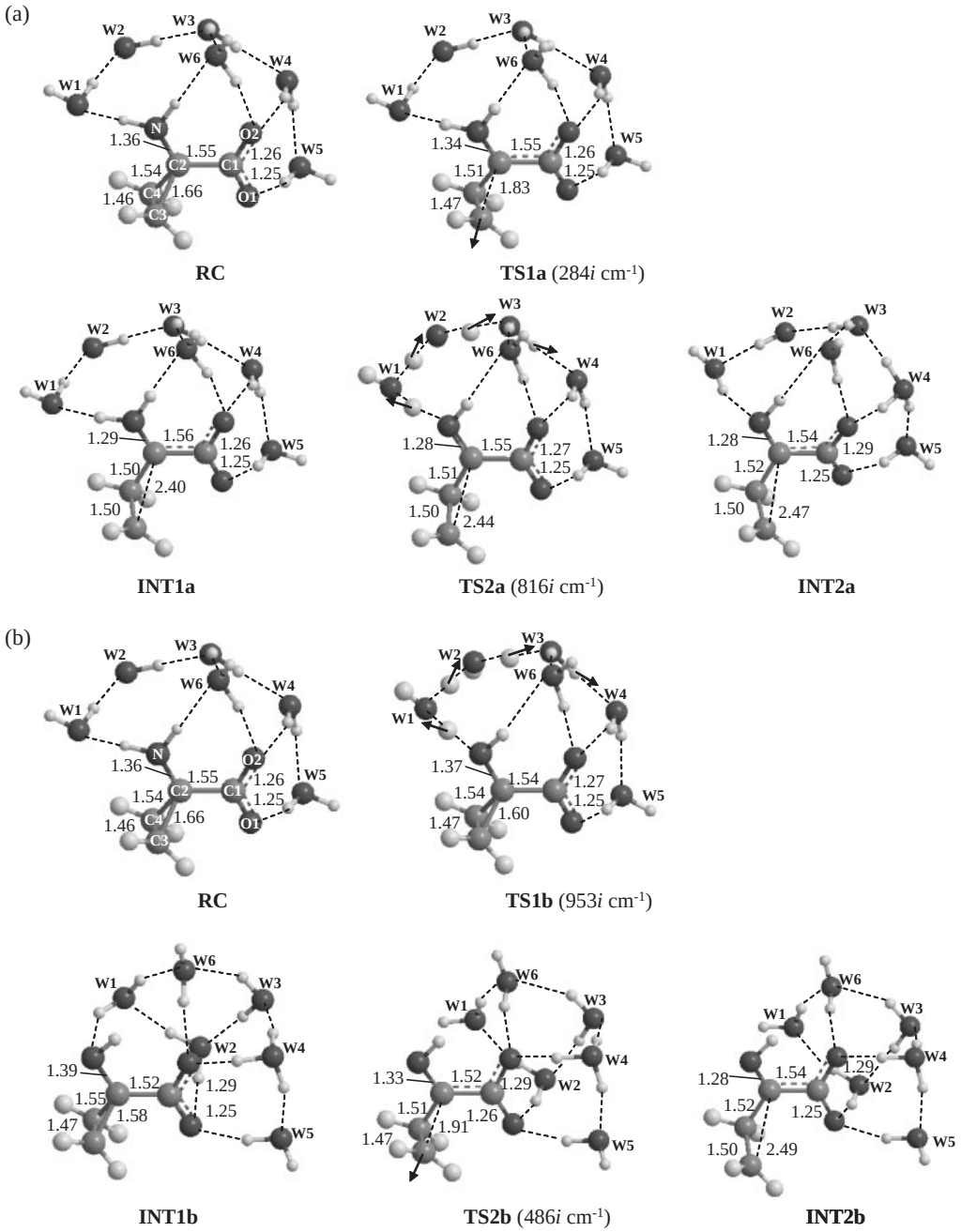

Fig. 2. Optimized geometries of the reactant (**RC**), transition-state (**TS**), and intermediate (**INT**) species for (a) Path A and (b) Path B from ACC amine radical cation in the hydrated cluster at the B3LYP/6-31+G(d,p) level. Bond lengths are shown in Å. The water molecules in the hydrated cluster are labeled with W1-6.

the atomic charges of the solute were also calculated as shown in Tables 3 and 5. The highest spin density was obtained at **N** of **RC**, **N** of **TS1b**, **N** of **INT1b**, **C3** of **TS2b**, and **C3** of **INT2b** in the atoms of the each structure of Path B, indicating that a radical is formed at these atoms. The charges of **N** of **RC** were positive (+0.38 and +0.53 at the B3LYP/6-31+G(d,p) and MP2/6-31+G(d,p) levels, respectively), whereas those of **N** of **INT1b** were almost zero. These calculated spin densities and charges indicate that, from **RC** to **INT1b**, the electronic aspect of the solute changes from an amine radical cation to an aminyl radical due to the proton transfer.

From the results of Path A and Path B, it is thought that water molecules could play roles not only as components of the hydrogen-bonding network in the hydrated cluster but also as the carriers of protons. Moreover, it is clearly shown that the fragmentation of the cyclopropane ring in Path A occurs by a stepwise mechanism through a free radical chain process, in agreement with experimental results,[13,14] and that the fragmentation of the cyclopropane ring in Path B also occurs by such a mechanism. In addition, almost the same bond lengths, spin densities, and charges were determined for **INT2a** of Path A and **INT2b** of Path B. Therefore, the carbon-centered radical product (carbon-centered radical 2 in Scheme 1) can be obtained not only by Path A but also by Path B, whereas an early

Table 2. Atomic Spin Densities and Atomic Charges of the Reactant (**RC**), Transition-State (**TS**), and Intermediate (**INT**) Species for Path A of Ethylene Formation from ACC Amine Radical Cation in the Hydrated Cluster Calculated at the B3LYP/6-31+G(d,p) Level

		RC	TS1a	INT1a	TS2a	INT2a
Spin density	**N**	0.59	0.44	0.04	0.03	0.03
	C1	0.01	0.01	0.04	0.04	0.04
	C2	0.02	0.01	0.07	0.05	0.06
	C3	0.33	0.59	1.11	1.13	1.15
	C4	0.05	−0.04	−0.21	−0.20	−0.21
	O1	0.05	0.04	0.01	0.00	0.00
	O2	−0.01	−0.01	0.00	0.00	0.00
Charge[a)]	**N**	0.38	0.33	0.35	−0.25	−0.21
	C1	0.23	0.22	0.17	0.09	0.29
	C2	0.31	0.36	0.38	0.37	0.16
	C3	0.18	0.17	0.09	0.07	0.04
	C4	0.18	0.20	0.23	0.24	0.26
	O1	−0.59	−0.60	−0.57	−0.58	−0.58
	O2	−0.69	−0.69	−0.68	−0.70	−0.75

a) The atomic charges with hydrogens summed into heavy atoms.

Table 3. Atomic Spin Densities and Atomic Charges of the Reactant (**RC**), Transition-State (**TS**), and Intermediate (**INT**) Species for Path B of Ethylene Formation from ACC Amine Radical Cation in the Hydrated Cluster Calculated at the B3LYP/6-31+G(d,p) Level

		RC	TS1b	INT1b	TS2b	INT2b
Spin density	**N**	0.59	0.74	0.86	0.58	0.03
	C1	0.01	0.02	0.04	0.07	0.02
	C2	0.02	−0.06	−0.11	−0.18	0.06
	C3	0.33	0.23	0.17	0.65	1.16
	C4	0.05	0.06	0.05	−0.07	−0.21
	O1	0.05	0.03	0.01	0.01	0.01
	O2	−0.01	−0.01	0.00	−0.01	0.00
Charge[a)]	**N**	0.38	−0.16	−0.09	−0.12	−0.12
	C1	0.23	0.24	0.17	0.12	0.09
	C2	0.31	0.19	−0.04	0.14	0.19
	C3	0.18	0.19	0.17	0.07	−0.03
	C4	0.18	0.16	0.27	0.40	0.44
	O1	−0.59	−0.61	−0.64	−0.69	−0.66
	O2	−0.69	−0.73	−0.75	−0.79	−0.79

a) The atomic charges with hydrogens summed into heavy atoms.

experimental study[17] has shown that the stable carbon-centered radical cannot be obtained by the ring opening of cyclopropylaminyl radical, which is analogous to ACC aminyl radical in Path B.

Energy Profiles: Figure 3 shows the relative energies without (ΔE) and with (ΔE_{ZPC}) zero-point vibrational correction and the corresponding free energy difference (ΔG) of the **RC**, **TS**, and **INT** species calculated at the B3LYP/6-31+G(d,p) level. As shown in Fig. 3, although the carbon-centered radical products (carbon-centered radical 2 in Scheme 1) were obtained through both of Path A (**INT2a**) and Path B (**INT2b**) with almost the same stabilities, the potential energy curves of Path A and Path B were different. To examine energetic details of Path A and Path B, the energy profiles of the proton-transfer and ring-opening processes of these paths were compared with each other.

Calculated barrier heights (ΔE) for the proton transfers from the amino group of **INT1a** in Path A (**TS2a**) and from that of **RC** in Path B (**TS1b**) were 11.97 and 11.42 kcal mol^{-1}, respectively, and these barrier heights were similarly reduced by the zero-point vibrational correction (by 4.13 and 4.18 kcal mol^{-1}, respectively), though they were not reduced by the effect of entropy. In addition, calculated reaction heats (ΔE) for the proton transfers from the amino group of **INT1a** in Path A and from that of **RC** in Path B were 3.26 and 2.83 kcal mol^{-1}, respectively, and these reaction heats were reduced by the zero-point vibrational correction (by 1.03 and 0.22 kcal mol^{-1}, respectively), though they were not reduced

Table 4. Atomic Spin Densities and Atomic Charges of the Reactant (**RC**), Transition-State (**TS**), and Intermediate (**INT**) Species for Path A of Ethylene Formation from ACC Amine Radical Cation in the Hydrated Cluster Calculated at the MP2/6-31+G(d,p) Level[a)]

		RC	TS1a	INT1a	TS2a	INT2a
Spin density	**N**	0.90	0.61	0.06	0.07	0.12
	C1	0.04	0.03	0.01	0.01	0.02
	C2	−0.25	−0.23	−0.01	−0.04	−0.08
	C3	0.43	0.90	1.43	1.44	1.43
	C4	0.02	−0.17	−0.31	−0.30	−0.31
	O1	0.02	0.03	0.00	0.00	0.00
	O2	−0.01	−0.02	0.00	0.00	0.00
Charge[b)]	**N**	0.53	0.40	0.39	−0.28	−0.22
	C1	0.61	0.59	0.52	0.45	0.51
	C2	0.19	0.28	0.29	0.23	0.09
	C3	0.16	0.15	0.07	0.06	0.07
	C4	0.10	0.14	0.23	0.26	0.27
	O1	−0.74	−0.73	−0.69	−0.70	−0.69
	O2	−0.85	−0.83	−0.81	−0.85	−0.90

a) The single point MP2 calculations using the optimized geometries in the hydrated cluster by the B3LYP calculations. b) The atomic charges with hydrogens summed into heavy atoms.

Table 5. Atomic Spin Densities and Atomic Charges of the Reactant (**RC**), Transition-State (**TS**), and Intermediate (**INT**) Species for Path B of Ethylene Formation from ACC Amine Radical Cation in the Hydrated Cluster Calculated at the MP2/6-31+G(d,p) Level[a)]

		RC	TS1b	INT1b	TS2b	INT2b
Spin density	**N**	0.90	1.05	1.07	0.90	−0.03
	C1	0.04	0.05	0.09	0.12	−0.01
	C2	−0.25	−0.30	−0.28	−0.65	0.09
	C3	0.43	0.27	0.19	1.01	1.32
	C4	0.02	0.05	0.02	−0.18	−0.20
	O1	0.02	0.01	0.00	−0.01	0.01
	O2	−0.01	−0.01	−0.01	−0.02	0.00
Charge[b)]	**N**	0.53	−0.07	−0.04	−0.06	−0.24
	C1	0.61	0.58	0.54	0.51	0.81
	C2	0.19	0.06	−0.10	0.00	0.16
	C3	0.16	0.16	0.19	0.07	0.06
	C4	0.10	0.10	0.18	0.34	0.04
	O1	−0.74	−0.75	−0.77	−0.81	−0.73
	O2	−0.85	−0.89	−0.95	−0.97	−0.87

a) The single point MP2 calculations using the optimized geometries in the hydrated cluster by the B3LYP calculations. b) The atomic charges with hydrogens summed into heavy atoms.

by the effect of entropy. This indicates that the proton transfers from the amino groups of carbon-centered radical 1 and ACC amine radical cation proceed with the similar barrier heights and the similar reaction heats in endothermic reaction mechanisms. In addition, the energy difference between **RC** and **INT1b** shows that ACC amine radical cation is more stable than ACC aminyl radical by 3.86 kcal mol^{-1} (ΔG).

The calculated barrier heights (ΔE) for the ring openings of the cyclopropane rings of **RC** in Path A (**TS1a**) and **INT1b** in Path B (**TS2b**) were 0.39 and 4.57 kcal mol^{-1}, respectively, and these barrier heights were slightly reduced by the zero-point vibrational correction (by 0.44 and 0.98 kcal mol^{-1}, respectively), though they were not reduced by the effect of entropy. Thus, the ring opening of **RC** proceeds with almost no barrier height, whereas that of **INT1b** proceeds with a higher barrier height. This result arises from the fact that the C2–C3 bond of **INT1b** is stronger than that of **RC**, as mentioned above. The calculated reaction heats (ΔE) for the cyclopropane rings of **RC** in Path A and **INT1b** in Path B were −4.27 and −3.92 kcal mol^{-1}, respectively, and both of **INT1a**

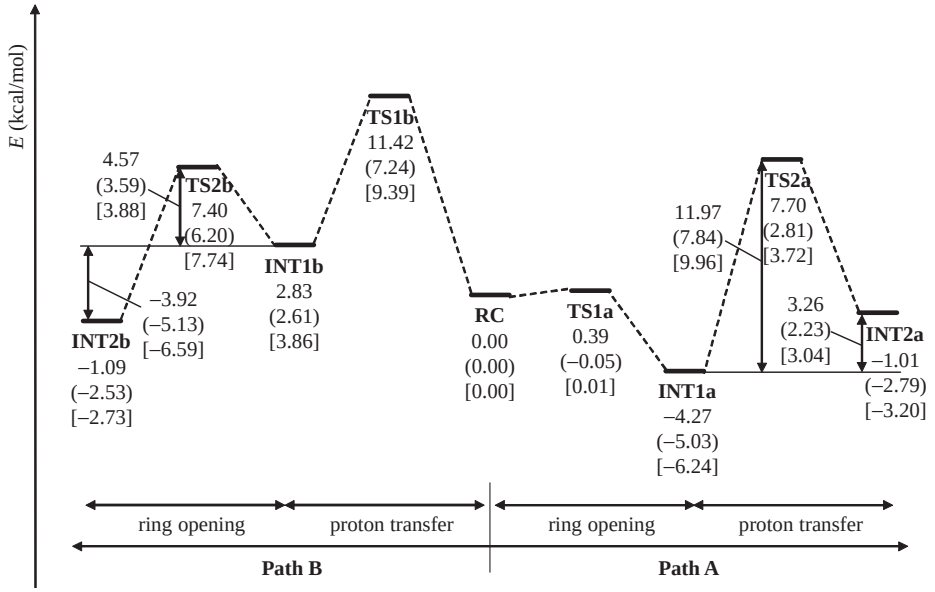

Fig. 3. Potential energy curves for Path A and Path B from ACC amine radical cation in the hydrated cluster at the B3LYP/6-31+G(d,p) level. Relative energies are shown in kcal mol^{-1}. The relative energies with zero-point vibrational correction and the corresponding free energy differences are also shown in round brackets ( ) and square brackets [ ], respectively.

and **INT2b** were similarly stabilized by the zero-point vibrational correction (by 0.76 and 1.21 kcal mol^{-1}, respectively) and the effect of entropy (by 1.21 and 1.46 kcal mol^{-1}, respectively). Thus, the ring openings of ACC amine radical cation and ACC aminyl radical proceed with the different barrier heights, though they proceed with the similar reaction heats in exothermic reaction mechanisms.

In addition, the rate constants (k) of these ring openings were estimated. In general, k for a reaction is given by the following equation based on transition-state theory[34–36]

$$k = \kappa\left(\frac{k_B T}{h}\right)e^{-\frac{\Delta G^{\ddagger}}{RT}}, \quad (1)$$

where κ is the transmission coefficient ($\kappa = 1$ for an adiabatic reaction), k_B is Boltzmann's constant, h is Planck's constant, R is the gas constant, T is the temperature, and $\Delta G^{\ddagger}$ is an activation free energy. As shown in the adiabatic potential energy curves for Path A and Path B (Fig. 3), the values of $\Delta G^{\ddagger}$ for the ring openings of ACC amine radical cation (**RC**) and ACC aminyl radical (**INT1b**) were 0.01 (**TS1a**) and 3.88 (**TS2b**) kcal mol^{-1}, respectively. Therefore, using Eq. 1, values of k of 6.10×10^{12} and 8.89×10^{9} s^{-1} at 298.15 K were estimated for the ring openings of ACC amine radical cation and ACC aminyl radical, respectively. These values show that both of the ring openings could occur with $k > 10^{8}$ s^{-1}, in agreement with experimental results.[13,14] Moreover, these values indicate that the ring opening of ACC amine radical cation occurs 10^{3}-fold faster than that of ACC aminyl radical. This computational estimation agrees with experimental estimation that amine radical cations can undergo rearrangements up to 10^{3}-fold faster than their cognate aminyl radicals.[15] Therefore, the barrier heights and rate constants of the ring openings of ACC amine radical cation and ACC aminyl radical were reasonably predicted by our calculations.

From the calculated barrier heights and reaction rate constants, it is clear that a remarkable difference between Path A and Path B appears in the ring-opening processes. Basically, the ring-opening process of ACC amine radical cation appears to proceed more readily than that of ACC aminyl radical, and once ACC amine radical cation is formed, its ring would spontaneously open with almost no barrier height. In other words, Path A is more favorable than Path B.

Conclusion

The stability and reactivity of ACC amine radical cation, which is a key intermediate of ethylene biosynthesis in plants, were examined by using quantum chemical calculations. The local interactions of ACC amine radical cation with water molecules in aqueous solution were treated with a hydrated cluster including six water molecules. It was found that the local interactions were necessary to stabilize ACC amine radical cation and to start its reaction. Potential energy curves were obtained for two types of reactions from ACC amine radical cation in the hydrated cluster: (1) direct ring opening of ACC amine radical cation, followed by proton abstraction from the amino group (Path A in Scheme 1), and (2) proton abstraction from the amino group, followed by ring opening of ACC aminyl radical (Path B in Scheme 1). A remarkable difference was found in the ring-opening processes of reactions (1) and (2). It was shown that the ring opening of ACC amine radical cation proceeded with almost no barrier height ($\Delta G = 0.01$ kcal mol^{-1} at the B3LYP/6-31+G(d,p) level), whereas that of ACC aminyl radical proceeds with a higher barrier height ($\Delta G = 3.88$ kcal mol^{-1} at the B3LYP/6-31+G(d,p) level). Rate constants (k) of 6.10×10^{12} and 8.89×10^{9} s^{-1} at 298.15 K were estimated for the ring openings of ACC amine radical cation and ACC aminyl radical, respectively, in agreement with the experimentally predicted value ($k > 10^{8}$ s^{-1}).[13,14] The computational finding that the ring opening of ACC amine radical cation proceeds 10^{3}-fold faster

than that of ACC aminyl radical agrees with experimental estimation for the analogous amine radical cations.[15] Taken together, it was quantitatively demonstrated that reaction (1) was more favorable than reaction (2). Therefore, ethylene synthesis should proceed predominantly through reaction (1). To our knowledge, this is the first report that examines these reaction mechanisms by comparing their barrier heights and reaction rate constants at the quantum mechanical level. The findings obtained from this work regarding the stability and reactivity of ACC amine radical cation would be useful for the eventual understanding of how ethylene is created in plants.

We thank Prof. Hiroshi Yamataka of Rikkyo University and Prof. Shigenori Tanaka of Kobe University for critical reading and comments on the manuscript, and Dr. Suyong Re of Ecole Normale Superieure for numerous helpful discussions.

References

1 D. Neljubow, *Beih. Bot. Zentralbl.* **1901**, *10*, 128.
2 S. F. Yang, N. E. Hoffman, *Annu. Rev. Plant Physiol.* **1984**, *35*, 155.
3 H. Kende, *Annu. Rev. Plant Physiol. Plant Mol. Biol.* **1993**, *44*, 283.
4 L. Alexander, D. Grierson, *J. Exp. Bot.* **2002**, *53*, 2039.
5 J. Kahl, D. H. Siemens, R. J. Aerts, R. Gäbler, F. Kühnemann, C. A. Preston, I. T. Baldwin, *Planta* **2000**, *210*, 336.
6 D. O. Adams, S. F. Yang, *Proc. Natl. Acad. Sci. U.S.A.* **1979**, *76*, 170.
7 M. C. Pirrung, *J. Am. Chem. Soc.* **1983**, *105*, 7207.
8 G. D. Peiser, T.-T. Wang, N. E. Hofmann, S. F. Yang, H.-W. Liu, C. T. Walsh, *Proc. Natl. Acad. Sci. U.S.A.* **1984**, *81*, 3059.
9 A. J. Hamilton, G. W. Lyett, D. Grierson, *Nature* **1990**, *346*, 284.
10 A. J. Hamilton, M. Bouzayen, D. Grierson, *Proc. Natl. Acad. Sci. U.S.A.* **1991**, *88*, 7434.
11 I. G. Dong, J. C. Fernandez-Maculet, S. F. Yang, *Proc. Natl. Acad. Sci. U.S.A.* **1992**, *89*, 9789.
12 M. C. Pirrung, L. M. Kaiser, J. Chen, *Biochemistry* **1993**, *32*, 7445.
13 M. C. Pirrung, J. Cao, J. Chen, *Chem. Biol.* **1998**, *5*, 49.
14 M. C. Pirrung, *Acc. Chem. Res.* **1999**, *32*, 711.
15 J. H. Horner, F. N. Martinez, O. M. Musa, M. Newcomb, H. E. Shasin, *J. Am. Chem. Soc.* **1995**, *117*, 11124.
16 O. M. Musa, J. H. Horner, H. Shasin, M. Newcomb, *J. Am. Chem. Soc.* **1996**, *118*, 3862.
17 X.-Z. Qin, F. Williams, *J. Am. Chem. Soc.* **1987**, *109*, 595.
18 D. Griller, K. U. Ingold, *Acc. Chem. Res.* **1980**, *13*, 317.
19 M. Ito, S. Re, H. Tokiwa, *J. Phys. Chem. A* **2004**, *108*, 5417.
20 I. A. Topol, S. K. Burt, A. A. Rashin, *Chem. Phys. Lett.* **1995**, *247*, 112.
21 J. J. Novoa, C. Sosa, *J. Phys. Chem.* **1995**, *99*, 15837.
22 S. Sadhukhan, D. Muñoz, C. Adamo, G. E. Scuseria, *Chem. Phys. Lett.* **1999**, *306*, 83.
23 C. Lee, W. Yang, R. G. Parr, *Phys. Rev. B* **1988**, *37*, 785.
24 A. D. Becke, *J. Chem. Phys.* **1993**, *98*, 1372.
25 A. D. Becke, *J. Chem. Phys.* **1993**, *98*, 5648.
26 C. Møller, M. S. Plesset, *Phys. Rev.* **1934**, *46*, 618.
27 P. M. Wojciechowski, W. Zierkiewicz, D. Michalska, P. Hobza, *J. Chem. Phys.* **2003**, *118*, 10900.
28 A. V. Marenich, J. E. Boggs, *J. Chem. Phys.* **2003**, *119*, 3098.
29 P. C. Hariharan, J. A. Pople, *Theor. Chim. Acta* **1973**, *28*, 213.
30 T. Clark, J. Chandrasekhar, G. W. Spitznagel, P. v. R. Schleyer, *J. Comput. Chem.* **1983**, *4*, 294.
31 K. Fukui, *Acc. Chem. Res.* **1981**, *14*, 363.
32 S. Mierts, E. Scrocco, J. Tomasi, *Chem. Phys.* **1981**, *55*, 117.
33 M. J. Frisch, G. W. Trucks, H. B. Schlegel, G. E. Scuseria, M. A. Robb, J. R. Cheeseman, V. G. Zakrzewski, J. A. Montgomery, Jr., R. E. Stratmann, J. C. Burant, S. Dapprich, J. M. Millam, A. D. Daniels, K. N. Kudin, M. C. Strain, O. Farkas, J. Tomasi, V. Barone, M. Cossi, R. Cammi, B. Mennucci, C. Pomelli, C. Adamo, S. Clifford, J. Orchterski, G. A. Petersson, P. Y. Ayala, Q. Cui, K. Morokuma, D. K. Malick, A. D. Rabuck, K. Raghavachari, J. B. Foresman, J. Cioslowski, J. V. Ortiz, B. B. Stefanov, G. Liu, A. Liashenko, P. Piskorz, I. Komaroni, R. Gomperts, R. L. Martin, D. J. Fox, T. Keith, M. A. Al-Laham, C. Y. Peng, A. Nanayakkara, C. Gonzalez, M. Challacombe, P. M. Gill, P. Johnson, W. Chen, M. W. Wong, J. L. Andres, M. Head-Gordon, E. S. Replogle, J. A. Pople, *Gaussian 98, Revision A.7*, Gaussian, Inc., Pittsburgh, PA, **1998**.
34 D. G. Truhlar, B. C. Garret, *Acc. Chem. Res.* **1980**, *13*, 440.
35 D. G. Truhlar, A. D. Isaacson, R. T. Skodje, B. C. Garret, *J. Phys. Chem.* **1982**, *86*, 2252.
36 D. G. Truhlar, B. C. Garret, S. J. Klippenstein, *J. Phys. Chem.* **1996**, *100*, 12771.
37 Detoxification of HCN is done through metabolic detoxification pathways in vivo, though it is formed as the byproduct of ethylene biosynthesis (Ref. 14).